Objective ARX Model Order Selection for Multi-Channel Human Operator Identification

Roggenkämper, N; Pool, DM; Drop, Frank; van Paassen, Rene; Mulder, M

DOI
10.2514/6.2016-4299

Publication date
2016

Document Version
Accepted author manuscript

Published in
Proceedings of the AIAA modeling and simulation technologies conference

Objective ARX Model Order Selection for Multi-Channel Human Operator Identification

N. Roggenkämper,* D.M. Pool,† F.M. Drop,‡ M.M. van Paassen,§ and M. Mulder¶
Delft University of Technology, Delft, The Netherlands

In manual control, the human operator primarily responds to visual inputs but may elect to make use of other available feedback paths such as physical motion, adopting a multi-channel control strategy. Human operator identification procedures generally require *a priori* selection of the model structure, which can be problematic as the exact feedback organization operators adopt is not always clear in advance. This paper evaluates a novel method for objectively detecting the presence of additional human operator feedback responses in control tasks with multiple inputs. The approach makes use of linear-time invariant ARX models for system identification, combined with an objective model selection criterion. To test the method, an experiment was conducted in which participants performed a compensatory yaw attitude tracking task in a moving-base flight simulator, with varying motion cueing settings. In addition, a pursuit tracking condition without motion feedback was tested. For all conditions, the objective ARX model-based identification method was used to verify the presence of a possible additional human operator output feedback response. With appropriate tuning of the penalty on model complexity in the model selection criterion, the methodology proved successful in correctly identifying the additional operator responses in experimental conditions that contained no motion or high-quality motion feedback. With low-fidelity motion feedback or a pursuit display, the results suggest that no consistent feedback response is achieved by the participants. The approach was substantiated with offline Monte Carlo simulations, which show strong correlation with the obtained experiment results.

Nomenclature

A, B	ARX model polynomials	K_n	Remnant intensity
a_k	ARX model denominator coefficient	K_p	Operator gain
b_k	ARX model numerator coefficient	k	Sample time, s
c	Penalty parameter for model complexity	N	Number of samples
d	Number of free parameters	n, w	Remnant signal, deg
e	Tracking error signal, deg	n_a	ARX model denominator order
f_d	Disturbance signal, deg	n_b	ARX model numerator order
F_n	Noise intensity level	n_k	ARX input time shift
f_t	Target signal, deg	q	Time shift operator
H_c	Controlled element dynamics	t	Time, s
H_{mf}	Motion filter dynamics	T_L	Operator lead time constant, s
H_{nm}	Neuromuscular dynamics	u	Human operator control signal, deg
H_n	Remnant filter dynamics	x	Controlled element output signal, deg
H_p	Human operator dynamics		
K_{mf}	Motion filter gain		

*MSc Student, Control and Simulation Section, Faculty of Aerospace Engineering, P.O. Box 5058, 2600GB Delft, The Netherlands; n.roggenkamper@student.tudelft.nl

†Assistant Professor, Control and Simulation Section, Faculty of Aerospace Engineering, P.O. Box 5058, 2600GB Delft, The Netherlands; d.m.pool@tudelft.nl. Member AIAA.

‡PhD Student, Max Planck Institute for Biological Cybernetics, Department Human Perception, Cognition and Action, Spemannstr. 38 - 44, 72076 Tübingen, Germany; frank.drop@tuebingen.mpg.de.

§Associate Professor, Control and Simulation Section, Faculty of Aerospace Engineering, P.O. Box 5058, 2600GB Delft, The Netherlands; m.m.vanpaassen@tudelft.nl. Member AIAA.

¶Professor, Control and Simulation Section, Faculty of Aerospace Engineering, P.O. Box 5058, 2600GB Delft, The Netherlands; m.mulder@tudelft.nl. Associate Fellow, AIAA.

Symbols

δ	Stick deflection, deg
ω_{mf}	Motion filter break frequency, rad/s
ω_n	Remnant break frequency, rad/s
ω_{nm}	Neuromuscular natural frequency, rad/s
ψ	Yaw attitude, deg
τ	Time delay, s
ζ_n	Remnant damping coefficient
ζ_{nm}	Neuromuscular damping coefficient

Subscripts

e	Human operator error response
x	Human operator output response

I. Introduction

Fundamental research carried out by McRuer et al.[1,2] in the 1960s still forms the basis for the mathematical modeling of pilot-vehicle systems today. Expressing human skills in the same control engineering terms as the vehicle to be controlled enables scientists to quantitatively evaluate human operators' manual control behavior. Decades of research have not only proven the validity of functional models as accurate descriptions of human tracking behavior during compensatory tracking tasks,[2–5] but also the suitability of system identification methods for human operator identification and modeling.[2,6–9]

For highly simplified control tasks, such as single-axis compensatory tracking tasks, human operator identification is relatively straightforward.[1,2] However, most realistic control tasks are more complex and involve multiple inputs, such as motion or additional visual information. To account for operators' use of different perceptual variables in a functional model, many researchers use a multi-channel human operator model structure,[6,10,11] demanding specific human operator identification procedures.[7–9] These multi-channel identification techniques require *a priori* definitions of the model structure, which implies that assumptions on which modalities operators actually respond to have to be made. In past research, the selection of the human operator control organization has entirely been based on previous empirical observations. For pursuit[12,13] tracking tasks and for control tasks including motion feedback,[6,14,15] it has been observed that the human operator often adopts a multi-channel control strategy.

However, it is not always clear in advance which responses the human operator actually makes use of. Recent experiments have shown that the human operator does not utilize additional motion feedback that has been distorted through application of high-pass motion filters.[16,17] Similarly, investigations including *ab initio* training experiments[18,19] revealed that the human operator might only develop an additional motion feedback response after extensive training. Also, Pool et al.[16] report only modest contributions of motion to operator control behavior in tasks with low-fidelity motion feedback, which even cast doubts on the presence of an additional motion feedback response. Selecting a multi-channel feedback organization in these cases could potentially lead to the identification of incorrect human operator dynamics. To increase our understanding of human operation during manual control, an objective human operator identification method that can extract the correct dynamics of the pilot-vehicle system would clearly be of significant scientific and engineering use.

This paper evaluates a novel method for including the objective detection of additional human operator feedback responses in human operator identification procedures. State-of-the-art research by Drop et al.[20] proposes a systematic approach that uses linear-time invariant models, in this case AutoRegressive eXogenous (ARX) models, for system identification in combination with an objective model selection criterion. To evaluate the fits of identified models, selection criteria that weigh the modeling quality against the model complexity, such as the Akaike information criterion (AIC)[21] or the Bayesian information criterion (BIC),[22] are commonly applied. For ARX models, the presence of operator responses is directly coupled to the order – i.e., the total number of parameters – of the selected models. Data from human-in-the-loop experiments is inherently noisy which could easily lead to overfitting and the wrong detection of an additional feedback response.[13,20] Drop et al. therefore proposed to modify the conventional BIC to include an increased penalty on the model complexity.

Drop et al.[20] previously applied this methodology to multi-channel control tasks with feedback and feedforward responses enabled by predictable reference signals. In this study, the same approach is applied to compensatory control tasks with motion feedback and to pursuit tracking tasks, to verify the utilization of the additional feedbacks in these applications. This includes verifying the tuning of the additional model complexity penalty proposed in Ref. 20, which is expected to be needed given the very different task and human operator control dynamics. This tuning of the method is performed and tested using both offline Monte Carlo simulations and a human-in-the-loop experiment, performed in TU Delft's SIMONA Research Simulator.

The paper is structured as follows. In Section II, the multi-channel control task to be investigated is introduced. Furthermore, the application of ARX models and the model selection criterion to this identification problem are described. Section III presents the methods, that is a human-in-the-loop experiment and offline Monte Carlo simulations,

that were used to generate data for testing the proposed identification approach. The results of application of the methodology to this data are analyzed in Section IV. Finally, the results are discussed and conclusions are drawn in Sections V and VI.

II. System Identification and Model Selection

II.A. Identification Problem

The schematic representations of the two multi-channel control tasks investigated in this paper are given in Figs. 1 and 2. Our compensatory control task with motion feedback is shown in Fig. 1a and the corresponding visual display in Fig. 1b. Although the human controller is a nonlinear system, for constant task conditions and with training, the operator's control action can be expressed by quasi-linear describing functions, in this case H_{p_e} and H_{p_x}, plus a remnant n which accounts for the nonlinearities.[2] The human operator controls a system with dynamics given by H_c through feedback of the tracking error e and, possibly, through additional feedback of the controlled element output x. In this study, the inputs to the controlled element were given by means of a sidestick with deflection δ. The dynamics of a motion filter that was applied to vary motion feedback quality are indicated by H_{mf}. H_{p_x} represents the additional output feedback response – i.e., a response to the controlled element output x – that the human operator may elect to make use of in tasks including motion feedback.[6,14,15]

However, it is known that human operators may also develop an output response when additional visual feedback is provided instead of motion.[12,13] A pursuit tracking task was included in this investigation to detect the presence of the H_{p_x} response in these tasks. On a pursuit display (Fig. 2b) the operator can observe the target signal f_t, the controlled element output x and the tracking error e, whereas on a compensatory display (Fig. 1b), only the tracking error e is shown to the operator. As done in previous studies,[12,13] for pursuit the same multi-channel structure as for a compensatory task with motion was assumed, with the only difference being the absence of the motion filter (see Fig. 2a).

Figs. 1a and 2a illustrate that the human operator tracks the target signal f_t and rejects the disturbance imposed by the signal f_d. The use of two forcing functions is necessary for separating the contributions of H_{p_e} and H_{p_x} when applying multi-channel human operator identification.[9]

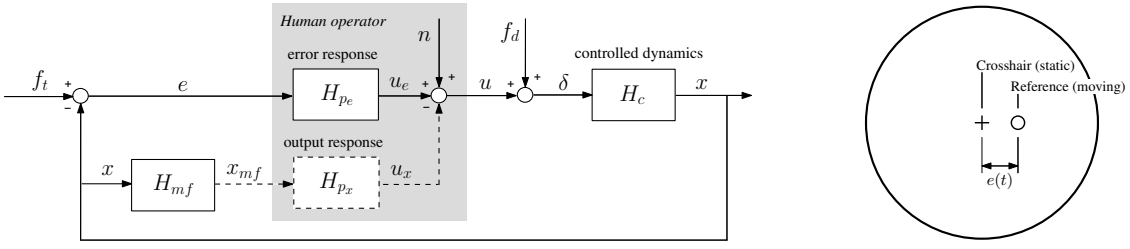

(a) Multi-channel compensatory control task. (b) Compensatory display.

Figure 1. Schematic representation of a multi-channel control task including motion and corresponding visual display.

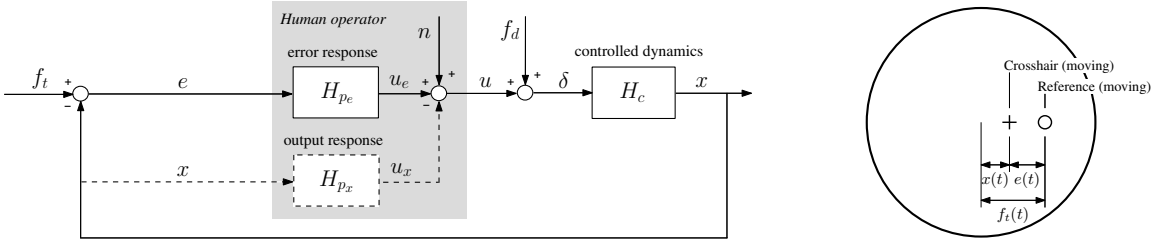

(a) Multi-channel pursuit control task. (b) Pursuit display

Figure 2. Schematic representation of a multi-channel pursuit control task and corresponding visual display.

System identification and parameter estimation methods that have successfully been applied to multi-channel human operator identification make use of Fourier coefficients (FC),[7,8] maximum likelihood estimation (MLE)[9,16,23,24] and linear-time invariant models (LTI).[8,13,25] While the approach described in this paper is primarily based on LTI

models, the MLE technique was used to estimate model parameters needed to set up the offline analysis (see Section III.C), and the FC method was applied to verify the identified LTI models.

II.B. System Identification using ARX Models

One often-applied approach to identify the human operator responses H_{p_e} and H_{p_x} from measured data makes use of linear-time invariant ARX models.[8] The suitability of ARX models for multi-channel human operator identification has been shown in previous research.[8,13,25] The ARX model structure has been applied in this study since its parameters can be determined directly from an analytical least-squares solution, but more complex LTI model structures such as Box-Jenkins and ARMAX can be applied in an analogous manner.[26] The multi-input-single-output (MISO) ARX model structure that can be used for identifying H_{p_e} and H_{p_x} (see Figs. 1a and 2a) is illustrated in Fig. 3.

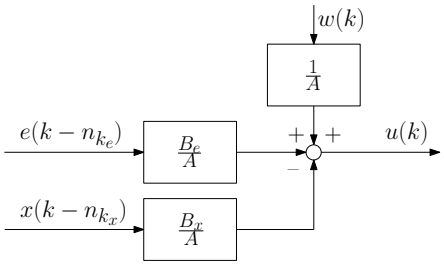

Figure 3. Multi-channel ARX model structure.

The model structure in Fig. 3 is equivalent to the human operator model indicated by the gray box in Figs. 1a and 2a, thus the operator response functions H_{p_e} and H_{p_x} are modeled by B_e/A and B_x/A, respectively. The terms n_{k_e} and n_{k_x} capture human processing delays (number of samples of input delay) and k the discrete sample time. Note that the remnant is represented by discrete-time white noise $w(k)$ which is passed through the ARX model denominator, causing the noise dynamics to be linked to the linear model estimates. With this assumption, the fit of an ARX model is conveniently obtained from an analytical least-squares linear regression solution.[26]

The time difference equation corresponding to the ARX model structure can be expressed by:

$$A(q)u(k) = B_e(q)e(k-n_{k_e}) + B_x(q)x(k-n_{k_x}) + w(k) \tag{1}$$

with:

$$A(q) = 1 + a_1 q^{-1} + ... + a_{n_a} q^{-n_a} \tag{2}$$

$$B_e(q) = b_{e,0} + b_{e,1} q^{-1} + ... + b_{e,n_{b_e}} q^{-n_{b_e}+1} \tag{3}$$

$$B_x(q) = b_{x,0} + b_{x,1} q^{-1} + ... + b_{x,n_{b_x}} q^{-n_{b_x}+1} \tag{4}$$

In Eqs. (2)-(4), q is the discrete-time shift operator, and a_k, $b_{e,k}$ and $b_{x,k}$ denote the coefficients of the corresponding polynomials. The order of the polynomials A, B_e and B_x – that is n_a, n_{b_e} and n_{b_x} – is directly linked to the total number of model parameters and consequently, the model complexity. Generally, these polynomial orders as well as the number of human operator responses (represented by the channels in Figs. 1a and 2a) are selected *a priori*, based on existing knowledge of the dynamics to be identified.[8,26] Choosing too many model parameters or responses could lead to *overfitting* and the identification of non-existing dynamics. On the other hand, the selection of too few model parameters or responses would result in *underfitting* and the failure to identify existing dynamics. In particular for scenarios that involve uncertainty with respect to the feedback organization of the human controller the identification of erroneous dynamics is very likely.

II.C. Model Selection

Drop et al.[20] have investigated a systematic approach that evaluates a large number of possible ARX model orders in terms of relative model quality, thereby objectifying model structure and order selection. The proposed approach uses a modified version of the well-known Bayesian Information Criterion (BIC),[22] which explicitly weighs the model quality against its complexity. While more restrictive than other proposed criteria (e.g., AIC[21]), Drop et al. found that the conventional BIC does not sufficiently penalize model complexity for the identification of human operator dynamics, because of the inherently high noise levels involved. To reduce the risk of overfitting, Drop et al. proposed

to use an additional penalty parameter c on the model complexity term of the original BIC, yielding the "modified BIC" (mBIC):[20]

$$\text{mBIC} = \underbrace{\ln V}_{\text{quality-of-fit}} + \underbrace{c\frac{d\ln N}{N}}_{\text{model complexity}} \tag{5}$$

In Eq. (5), N represents the number of samples used for identification, and V is the mean squared error of the model output which is generally defined as:

$$V = \frac{1}{N}\sum_{k=1}^{N}(\hat{u}(k) - u(k))^2 \tag{6}$$

In Eq. (6), u is the human operator control output, while $\hat{u}$ is the output signal obtained by simulating the ARX model.

In the model complexity term of Eq. (5), d represents the number of free model parameters. For the ARX model structure of Fig. 3, d is defined as:

$$d = \begin{cases} n_a + n_{b_e} + n_{b_x} & \text{if} \quad n_{k_e} = 0 \text{ and } n_{k_x} = 0 \\ n_a + n_{b_e} + n_{b_x} + 1 & \text{if} \quad n_{k_e} = 0 \text{ or } n_{k_x} = 0 \\ n_a + n_{b_e} + n_{b_x} + 2 & \text{if} \quad n_{k_e} > 0 \text{ and } n_{k_x} > 0 \end{cases} \tag{7}$$

As is evident from Eq. (7), the number of parameters of an ARX model is strongly dependent on the sum of the orders of the A, B_e, and B_x polynomials, that is $n_a + n_{b_e} + n_{b_x}$. For models that do not include the additional output feedback response n_{b_x} is thus zero. As proposed by Drop et al.,[20] also nonzero time delay parameters (n_{k_e} and n_{k_x}) are included in the total model parameter count d. The subsequent analysis of experiment and simulation data will focus on the further required scaling on the model complexity term (c parameter) for this definition of d.

II.D. Approach

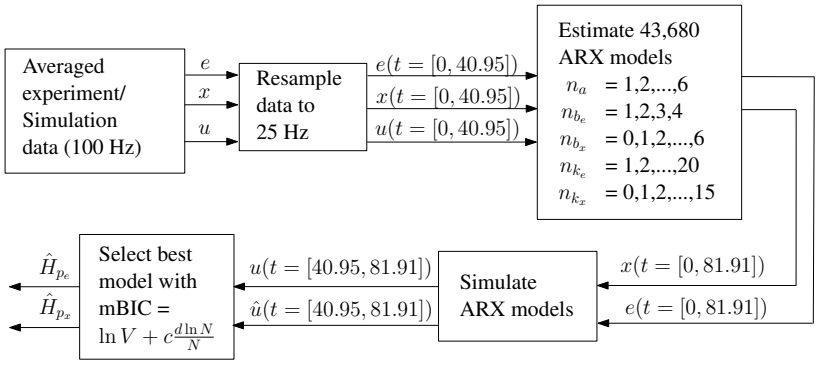

Figure 4. ARX model identification and model selection approach.

The proposed identification approach, which is schematically illustrated in Fig. 4, was tested on computer simulation and experiment data and is identical for both types of data. First, the time traces of the tracking error e, control output u and controlled element output x sampled at 100 Hz were resampled to 25 Hz, to reduce high-frequency noise and computational time in the steps that followed. A total of 43,680 ARX models were then fitted to the first half of the data. The number of models results from the combination of polynomial orders that were selected based on existing physical insight of human operator models. The ranges for the tested model parameters are provided in Fig. 4. For the model parameters associated with the output response H_{p_x}, zeros were included to cover the case when there is only an error response H_{p_e}.

Each estimated ARX model was simulated with the full dataset of measured input signals to obtain the estimated output signal. To find the best model fit, the proposed model selection criterion was then applied to the second half of the measured and estimated output signal. The optimal model corresponds to the model with the lowest mBIC value which depends on the magnitude of the c parameter. For the same measured data, a change in c could result in the identification of a different best model. Therefore, to evaluate the effect of the penalty parameter, optimal models

corresponding to a range of c values were determined for each dataset. The results could then be used to tune the c parameter which will be explained in Section IV.

The best model for a certain c setting does not necessarily provide the best possible quality-of-fit, due to the trade-off made between model complexity and quality. For comparison, and to evaluate the overall quality of all ARX model fits, the Variance Accounted For (VAF), given by Eq. (8), was also calculated as an intuitive and interpretable metric of fit quality. Once the best model and the corresponding parameters were known the operator response functions estimates $\hat{H}_{p_{e,x}} = B_{e,x}/A$ could be obtained.

$$\text{VAF} = \left(1 - \frac{\sum_{k=1}^{N}(\hat{u}(k) - u(k))^2}{\sum_{k=1}^{N}(u(k))^2}\right) \times 100\% \tag{8}$$

III. Methods

III.A. Control Task

The methodology introduced in this paper was tested on data collected in a human-in-the-loop experiment and simulation data obtained through an offline analysis. The control task was chosen to be a yaw attitude tracking task, similar to the one used by Lu et al.[24] to investigate the effect of yaw rotational motion on human operator behavior. Therefore, the output of the controlled element x in Figs. 1a and 2a is the yaw attitude ψ. The dynamics of the controlled element were given by a double integrator:

$$H_c(s) = \frac{K_c}{s^2} \tag{9}$$

The control of such dynamics requires significant human operator lead equalization and it has been observed that in this case the human operator does make use of additional physical motion feedback.[14] Since then the additional human operator output response is present, the approach can be tested for its capability in identifying the correct multi-channel human operator dynamics.

Both, a control task with physical motion feedback and a pursuit tracking task were tested, so the display configuration had to be adjusted during the experiment. The compensatory display shown in Fig. 1b was presented to the participants in all experimental conditions except the pursuit condition in which the pursuit display in Fig. 2b was used.

III.B. Human-In-The-Loop Experiment

Apparatus

The experiment was performed in the SIMONA Research Simulator (SRS) at Delft University of Technology (Fig. 5). The SRS has a hydraulic six-degree-of-freedom hexapod motion system that was used to provide the yaw motion feedback during the experiment. The time delay of the SRS motion system is 30 ms.[27] The compensatory or pursuit display was presented on a PFD in front of the participants and no other visual cues were provided. Participants gave control inputs by means of a Moog FCS Ecol-8000 electrical sidestick from the right seat in the simulator cab. The stiffness of the spring centered sidestick was set to 1.5 N/deg and the roll axis was used to give control inputs in yaw. The stick had no breakout force and deflections were limited to $\pm$ 15 deg. The pitch axis of the sidestick was locked at the zero position during the experiment.

Figure 5. The SIMONA Research Simulator.

Independent Variables

To compare our approach's capability to cope with varying strength of H_{p_x}, the two independent variables in the experiment were the amount of motion feedback supplied, as well as the two display configurations, compensatory or pursuit. The fidelity of the motion feedback was adjusted using a first-order high-pass washout filter as was done in previous investigations:[16,17]

$$H_{mf}(s) = K_{mf}\frac{s}{s+\omega_{mf}} \tag{10}$$

In Eq. (10), K_{mf} denotes the motion filter gain and ω_{mf} the filter break frequency. The five different experimental conditions and the corresponding motion filter settings are summarized in Table 1. For the first four conditions (C0-C3) the tracking task was presented on a compensatory display (see Fig. 1b) while the strength of the yaw motion feedback was varied from no motion to unfiltered one-to-one motion. The motion settings are based on an experiment conducted by Pool et al.[16] which showed that human operators develop an H_{p_x} response for high-fidelity (C2) and perfect motion (C3) feedback. However, for low-fidelity motion quality (C1) the presence of this response remained uncertain. The motion settings were adopted in this study to compare the strength of the output response for two conditions of good motion quality and to reassess the presence of H_{p_x} for low-fidelity motion feedback. Since for both, one-to-one motion and no motion (C0) the human operator control organization is known, these conditions serve as a valuable reference.

For the fifth condition (P0) the tracking task was presented on a pursuit display (see Fig. 2b) and no physical motion cues were supplied. Feedback provided by the additional visual cues on a pursuit display leads to an improvement in tracking performance,[12,13] although vestibular cues generally appear to have a greater effect.[28] Similar to control tasks with motion feedback it remains uncertain, however, whether an output response H_{p_x} is actually utilized. To revisit identification issues from earlier work[13,28] and to compare the strength of pursuit and motion effects, a pursuit tracking condition without motion feedback was included.

Table 1. Experimental conditions

Condition	Display setting	Motion setting	Motion gain K_{mf}, –	Motion break frequency ω_{mf}, rad/s
C0	compensatory	no motion	0.0	–
C1	compensatory	low-fidelity motion	0.5	0.5
C2	compensatory	high-fidelity motion	1.0	0.5
C3	compensatory	perfect motion	1.0	0.0
P0	pursuit	no motion	0.0	–

Forcing Functions

The disturbance and target forcing functions used were independent quasi-random sum-of-sines signals of equal power as applied in previous investigations for the identification of multi-channel human operator models in both, frequency and time domain.[6,9] Both signals consisted of ten sinusoids defined by:

$$f_{d,t}(t) = \sum_{k=1}^{10} A_{d,t}(k)\sin\left(\omega_{d,t}(k)t + \phi_{d,t}(k)\right) \tag{11}$$

In Eq. (11), $A_{d,t}$, $\omega_{d,t}$, and $\phi_{d,t}$ denote the amplitude, frequency and phase of the k^{th} sinusoid in the f_d or f_t signals. An approach that has been used in earlier studies for multi-channel human operator model identification employs Fourier coefficients[7,8] and was applied in this study for comparison and bilateral verification of the identified ARX models. Therefore, to permit the use of spectral methods, the forcing function frequencies were all defined as integer multiples of the measurement window base frequency $\omega_m = 2\pi/T_m$ with $T_m = 81.92$ s.

Table 2 provides the integer factors n_d and n_t as well as the forcing function amplitudes, frequencies, and phases. The forcing function properties are almost identical to those applied by Lu et al.[24] for a comparable yaw tracking control task. The only difference with Ref. 24 lies in the scaling of the target signal amplitudes A_t, which are reduced by 50% for our experiment so that the target and disturbance signals have the same strength.

Table 2. Forcing function properties

	disturbance, f_d				target, f_t			
k	n_d	ω_d	A_d	ϕ_d	n_t	ω_t	A_t	ϕ_t
-	-	rad/s	deg	rad	-	rad/s	deg	rad
1	5	0.383	2.057	-0.269	6	0.460	2.139	1.288
2	11	0.844	1.555	4.016	13	0.997	1.496	6.089
3	23	1.764	0.775	-0.806	27	2.071	0.675	5.507
4	37	2.838	0.395	4.938	41	3.145	0.363	1.734
5	51	3.912	0.240	5.442	53	4.065	0.244	2.019
6	71	5.446	0.146	2.274	73	5.599	0.151	0.441
7	101	7.747	0.091	1.636	103	7.900	0.096	5.175
8	137	10.508	0.066	2.973	139	10.661	0.070	3.415
9	171	13.116	0.055	3.429	194	14.880	0.055	1.066
10	226	17.334	0.047	3.486	229	17.564	0.050	3.479

Experimental Procedure

Five subjects performed the yaw attitude tracking task for the five conditions listed in Table 1. All participants had experience with similar tracking tasks from earlier simulator experiments. Their ages ranged from 25 to 53 years ($\mu =$ 31 years, $\sigma = 12.3$ years). Participants were instructed to minimize the yaw tracking error. For performance feedback the root mean square error was logged and reported to the test subjects after each run. All conditions (see Table 1) were tested in a single experiment session with regular breaks to avoid fatigue. Following a familiarization phase, a number of training runs were performed until control performance reached a consistent level, then five consecutive runs were collected as measurement data. On average, nine to ten tracking runs were performed for each condition. The experimental conditions were presented in a different randomized order for each subject (Latin square), as given in Table 3.

Table 3. Experiment matrix

Subject	Trial 1	Trial 2	Trial 3	Trial 4	Trial 5
1	C0	P0	C1	C2	C3
2	C2	C1	C3	P0	C0
3	C1	C0	C2	C3	P0
4	C3	C2	P0	C0	C1
5	P0	C3	C0	C1	C2

Hypotheses

Prior to the experiment, the presence and strength of the additional operator response H_{p_x} was hypothesized. For two of the experimental conditions listed in Table 1, the human operator control organization is known from extensive experimental investigations.[6,14,15] For condition C0, no additional feedback is provided to the operator except for e reducing the model to a single-channel control task, $H_{p_x} = 0$. On the other hand, with one-to-one motion feedback (condition C3) human operators have shown to develop a strong output response.[6,14–16] For the other conditions the following hypotheses were made:

1. Earlier studies revealed that human operators hardly utilize low-fidelity motion feedback,[16,17] so for condition C1 the H_{p_x} response was expected to be weak, if present at all.

2. The strength of the additional response for condition C2 was suspected to be very comparable to condition C3. Previous work found the motion contribution to the operator control output to be effectively the same for high-fidelity motion feedback conditions with the same gain.[16]

3. Based on the results of earlier investigations focusing on pursuit tracking,[13,28] for condition P0 the output response was expected to be less strongly present than for high-fidelity motion feedback.

The objective identification approach is based on recent research.[20] However, due to the similarity between the control tasks investigated, the applicability and effectiveness of the criterion was hypothesized to be comparable in

both studies. Still, the required value for the model complexity scaling factor c was not necessarily expected to be equal, thus requiring renewed tuning of the identification method.

III.C. Offline Simulations

Human Operator Model

The methodology proposed in this paper was tested in offline closed-loop Monte Carlo simulations of the multi-channel control tasks illustrated in Figs. 1 and 2. The same forcing function signals, controlled element dynamics and motion settings as used during the experiment were implemented in the simulation model. The model for the human operator error response H_{p_e} is based on McRuer et al.'s *precision model*[1] and is defined as follows:

$$H_{p_e}(s) = K_{p_e}(T_L s + 1)e^{-s\tau_e}H_{nm}(s) \tag{12}$$

The error response function in Eq. (12) consists of an equalization term given by $K_{p_e}(T_L s+1)$ where K_{p_e} denotes the error feedback gain and T_L the lead time constant, and a term representing the operator's limitations including the error feedback time delay $e^{-s\tau_e}$ and neuromuscular dynamics H_{nm}. The human operator tries to adjust his or her control strategy in such a way that the open-loop dynamics of the pilot-vehicle system approximate single-integrator dynamics.[1] For a controlled element with double-integrator dynamics, human operator lead equalization is expected, therefore the equalization term in Eq. (12) is a gain-lead element.[1] The output response function is given by:

$$H_{p_x}(s) = K_{p_x}se^{-s\tau_x}H_{nm}(s) \tag{13}$$

The model in Eq. (13) is a simplification of the human operator's response to the output x for control of double-integrator system dynamics which has been applied in previous research.[29,30] The equalization term $K_{p_x}s$ models human operator lead. The output feedback gain and time delay are K_{p_x} and $e^{-s\tau_x}$, respectively. The human neuromuscular dynamics can be modeled as a second-order mass-spring-damper system with damping ratio ζ_{nm} and undamped natural frequency ω_{nm}:[1]

$$H_{nm}(s) = \frac{\omega_{nm}^2}{s^2 + 2\zeta_{nm}\omega_{nm}s + \omega_{nm}^2} \tag{14}$$

To account for nonlinear contributions to the operator's output, a remnant signal is added that consists of Gaussian white noise passed through a third-order low-pass filter:[9]

$$H_n(s) = \frac{K_n\omega_n^3}{(s^2 + 2\zeta_n\omega_n s + \omega_n^2)(s + \omega_n)} \tag{15}$$

In Eq. (15), ω_n is the remnant break frequency and ζ_n the remnant damping coefficient. The values for the filter characteristics are given by ω_n = 12.7 rad/s and ζ_n = 0.26 as applied in earlier research.[9] The remnant intensity K_n was determined by means of nonlinear optimization to set the noise intensity level $F_n = \sigma_n^2/\sigma_u^2$. In total, 100 noise realizations were simulated for six different noise intensity levels (F_n = 0.05, 0.1, 0.15, 0.2, 0.25 and 0.3) and for each of the five experimental conditions.

Analysis Parameters and Settings

To create offline Monte Carlo simulations with human operator models matching the operator behavior observed in the experiment, representative model parameters were first estimated from the measured data. A total of seven model parameter values had to be found: the human operator model gains, K_{p_e} and K_{p_x}, time delays τ_e and τ_x, lead time constant T_L and the parameters of the neuromuscular dynamics model ω_{nm} and ζ_{nm}. For parameter estimation a time-domain parameter estimation technique was used, which has successfully been applied to multi-channel human operator identification before.[9,16,23,24] The obtained parameter values for each subject in our experiment can be found in Appendix A. Their mean values over the five subjects were used for the simulations and have been summarized in Table 4.

Both responses H_{p_e} and H_{p_x} were included in the analysis for all conditions except the compensatory no-motion condition C0. In contrast to the experiment, here the human control organization is known, which means that the simulation results can act as an important measure of the overall identification method's performance. As mentioned before, different noise intensity levels were included in the offline analysis to account for the variations in noise commonly found in measured data from human-in-the-loop experiments. By providing multiple scenarios the best match between experiment and simulation results can be found.

Table 4. Human operator model parameters used in the offline simulations.

Condition	Parameter						
	K_{p_e}	T_L	K_{p_x}	τ_e	τ_x	ω_{nm}	ζ_{nm}
	–	s	–	s	s	rad/s	–
C0	0.1240	1.3740	–	0.2448	–	10.7348	0.2359
C1	0.2776	0.5876	0.2086	0.2779	0.0891	11.2129	0.1668
C2	0.3747	0.3268	0.1795	0.3003	0.1072	11.7693	0.1867
C3	0.2899	0.3662	0.1767	0.3168	0.1223	11.8858	0.1406
P0	0.1107	1.2971	0.0381	0.2638	0.1995	10.6939	0.2234

IV. Results

IV.A. Experiment

Fig. 6 presents the results of application of the proposed identification method to the collected experiment data. In Fig. 6a the graphs indicate the percentage of identified models that contain an H_{p_x} response and that are optimal according to the mBIC criterion. The percentages are calculated over the average measurement data (5 runs) and the five participants and are then plotted for each condition against increasing values of c.

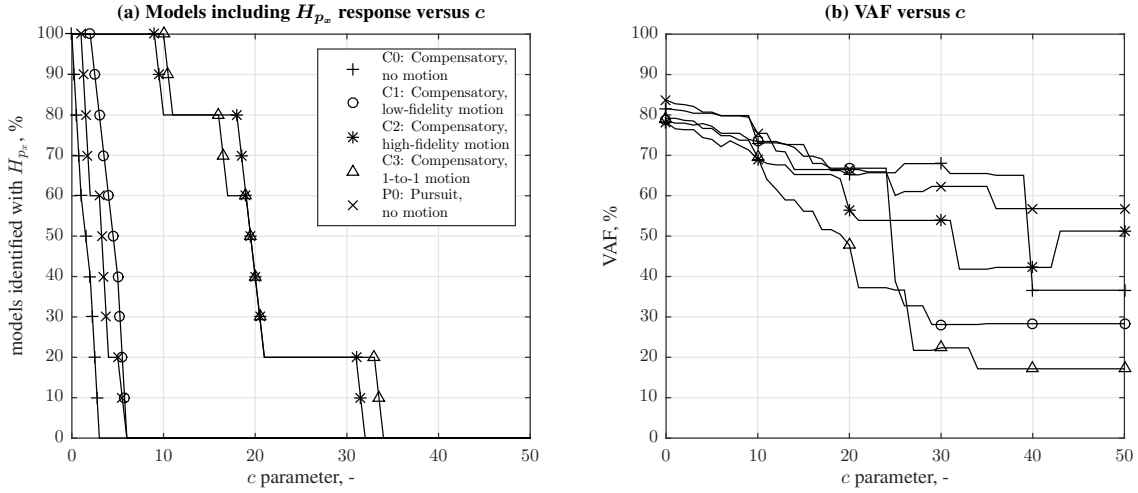

Figure 6. Results from averaged experiment data for all conditions.

Fig. 6a clearly shows that for higher c values less ARX models including an H_{p_x} response are identified, as the model complexity is increasingly penalized. Accordingly, the presence of an H_{p_x} response in the measured data becomes more likely the further the data for a condition is shifted to the right. Since there is no additional feedback provided to the operator in the no-motion condition (C0), here all identified models that include an output response are false-positives. As can be seen in Fig. 6a, false-positive models are no longer identified for $c > 3$. Note that for $c = 1$ the modified BIC criterion reduces to the conventional version of the BIC, but at this value a high percentage of incorrect models is identified for C0. These findings confirm that the original BIC indeed has to be modified to be effective in our application.

For conditions C2 and C3, with high-fidelity and perfect motion feedback, it was hypothesized that the human operator develops a strong H_{p_x} response[14] and as expected the corresponding graphs are offset well to the right compared to C0. For these conditions, exclusively models containing the output response should be identified. As can be verified from Fig. 6a, for $c > 9$ models without H_{p_x} (so, false-negatives) are found to provide an optimal fit in some cases, however. Combined with the results for C0, this suggests that for $3 < c < 10$ the mBIC criterion penalizes model complexity to the extent as to prevent false-negative identification of H_{p_x} for the no-motion task of C0, while also avoiding false-negatives and allowing for consistent identification of an H_{p_x} response for conditions with high-fidelity motion feedback (C2 and C3).

From Fig. 6a, there seems little evidence for an H_{p_x} response in the data of the pursuit (P0) and low-fidelity motion (C1) conditions. The data for these conditions are close to the C0 result, suggesting that human operators do not make effective use of the additional feedback provided in these conditions. Furthermore, for these two critical cases $3 < c < 10$ will result in inconsistent H_{p_x} response identification over our collected data: for some participants, an H_{p_x} response will be found, while for others its contribution is suppressed by the mBIC.

Fig. 6b shows the VAF for the models that were selected by the mBIC criterion versus the c parameter for all conditions. As expected, the VAF decreases with increasing c as the model complexity and therefore the descriptive capacity is increasingly penalized. It should be noted that the model selection criterion does not necessarily pick the best model fit (highest VAF) which explains slight fluctuations in the graph. The decreasing model quality seen in Fig. 6b implicates that an optimal c value should be selected as low as possible.

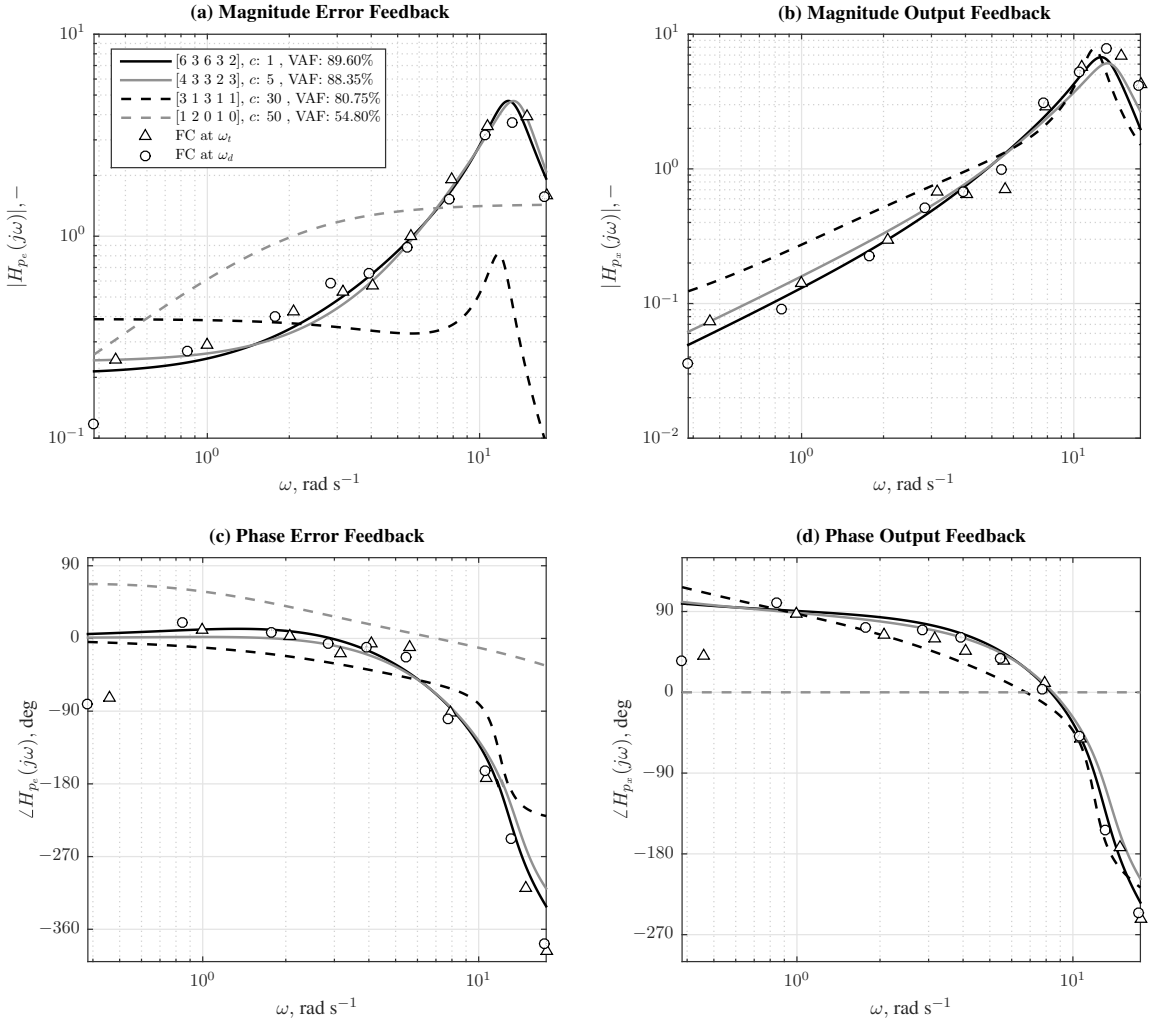

Figure 7. Bode plot of sample human operator identification results for Subject 3 and condition C3.

Fig. 7 shows a representative Bode plot for condition C3, Subject 3, and for four different c values. The model parameters (n_a,n_{b_e},n_{b_x},n_{k_e},n_{k_x}) and VAF corresponding to the c values have been included in the legend entries. To evaluate the quality of the obtained ARX models, the results from the identification with Fourier coefficients (FC) are illustrated in the same plot. They are indicated by the markers at the input frequencies of the forcing functions in Fig. 7. As can be seen, both identification techniques provide similar results. Since this condition includes motion feedback, the ARX model for $c = 50$ is a false-negative result, as $H_{p_x} = 0$ is shown in Figs. 7b and 7d. Also for $c = 30$ an erroneous ARX model result, with very low polynomial orders, that does not match the FC data is obtained. For $c = 3$, so within the identified "ideal" range of $3 < c < 10$, a highly satisfactory ARX result is found: the

obtained model has a lower parameter count than the $c = 1$ result, but still captures the human operator dynamics at high accuracy.

In Fig. 8a the percentage of models including an H_{p_x} response versus c is illustrated for condition C3, all subjects and averaged over the five measurement runs. The graphs present the data for the individual subjects to compare in-between subject variability. This "binary" single-subject data, averaged over all five subjects, results in the more gradual change with increasing c as shown in Fig. 6a. For reference, this average result is indicated in Fig. 8a with a thick gray line.

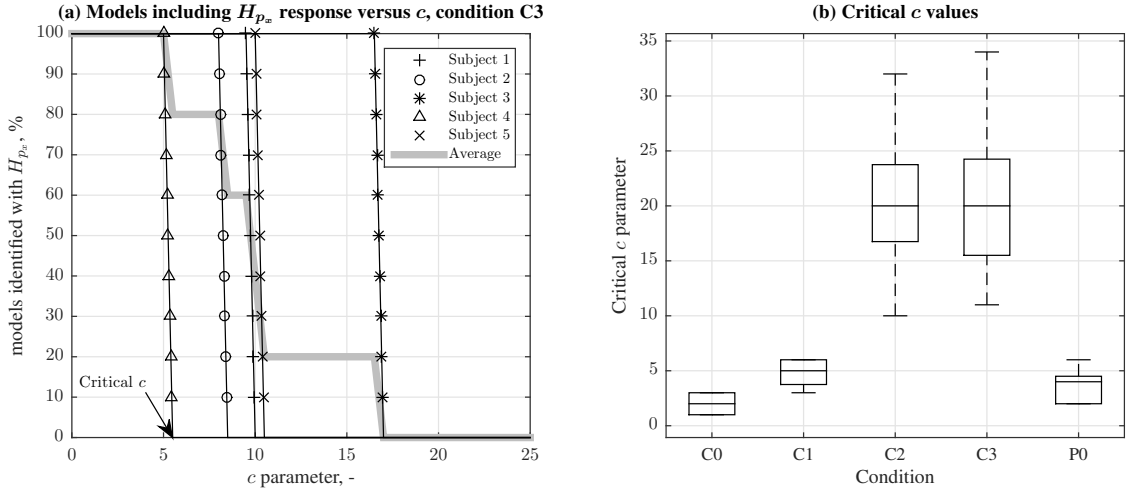

Figure 8. Identified H_{p_x} versus c for condition C3 and corresponding critical c values presented in a boxplot.

Fig. 8a shows that once a certain critical c value has been exceeded, models including an output response are no longer identified. This critical c value is indicated in the Fig. 8a for Subject 4. There is a wide spread of critical c values in this condition, which is reflected in the box plot shown in Fig. 8b. In this figure the edges of the boxes are the 25th and 75th percentiles and the central mark is the median. Fig. 8b clearly shows that conditions C2 and C3 are offset from the other conditions with a significantly higher critical c value. A one-way repeated measures analysis of variance (ANOVA) revealed that this effect was indeed statistically significant ($F(2.0,8.0)=15.77$ and $p < 0.05$).[a]

The relatively high critical c values found for the conditions with effective motion feedback confirms the results found in Fig. 6a and are strong evidence for the presence of an H_{p_x} response in these conditions.

IV.B. Simulations

The objective model selection procedure was also applied to simulation data. The results of this offline analysis are illustrated in Fig. 9. Again, the percentages of models with an output response are plotted against a range of increasing c parameters. The values indicated are the percentages over 100 noise realizations and for six different noise intensity levels. For comparison, the results from the analysis of the experiment data are indicated by the thick gray lines in the same figure. It should be noted that the scaling of the x-axes in Fig. 9a and Fig. 9e was adjusted for clarity.

The positions of the lines for the different noise intensity levels demonstrate the influence of noise on the identification of the modeled dynamics. The evidence for the additional feedback response in the data decreases the further the line shifts to the left. For condition C0 the true dynamics do not contain the output response, therefore a graph far to the left is most desirable. As the additional operator response was included in the simulations for all other conditions, the corresponding lines should preferably lie on the right. Fig. 9 demonstrates that for increasing levels of noise the graphs for the conditions including H_{p_x} are shifted to the left. This means that the remnant hides the additional response in these conditions. In contrast, for condition C0 in Fig. 9a the lines are shifted to the right for increasing noise intensities, implying that the remnant causes a false H_{p_x} response to appear.

As can be seen in Fig. 9 the results obtained for the experiment data are mostly in line with the simulation data results at noise intensity levels between 10 and 25% of the operator's control signal power, matching the remnant contribution expected for measured human operator behavior.[2,4,8,9] Table 5 lists the coefficient of determination (r^2)

[a] A Kolmogorov-Smirnov test found the data to be normally distributed, but Mauchly's test of sphericity showed that the assumption of sphericity was met. Hence, the Greenhouse-Geisser sphericity correction was applied.

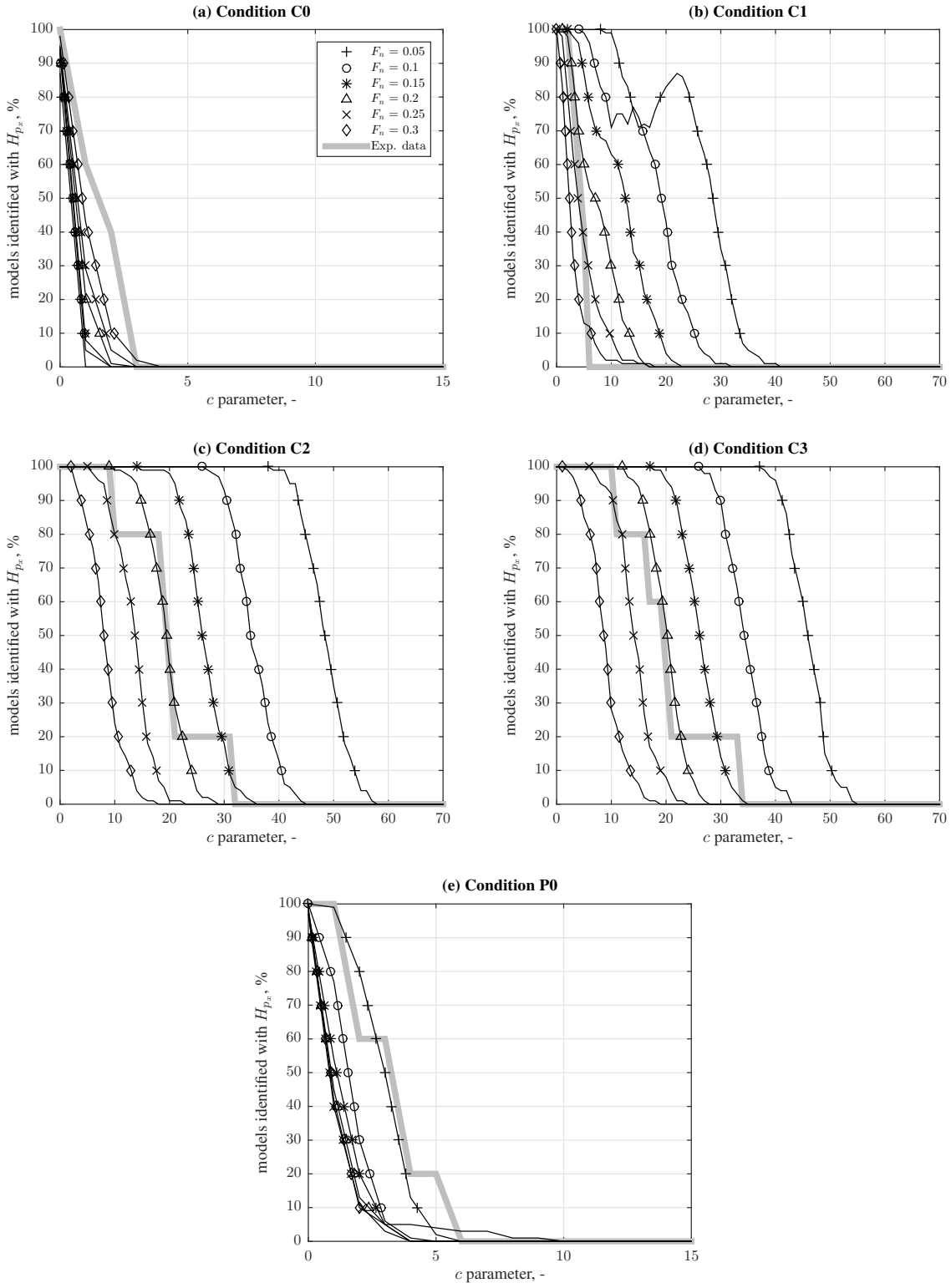

Figure 9. Identified H_{p_x} versus c for different noise intensity levels.

values between simulation and experiment data. The r^2 data shows that on average, simulations with F_n equal to 0.2-0.25 are most in line with the experiment data.

Table 5. Coefficients of determination (r^2) for experiment and simulation data with different F_n. Bold values indicate the highest r^2 for each condition.

Condition	F_n, -					
	0.05	0.1	0.15	0.2	0.25	0.3
C0	0.6559	0.6970	0.7196	0.8101	0.8691	**0.9329**
C1	0.2136	0.3631	0.5598	0.7947	**0.9415**	0.8737
C2	0.4117	0.6688	0.8728	**0.9706**	0.8265	0.6013
C3	0.4645	0.6996	0.8617	**0.9626**	0.8846	0.6514
P0	**0.9687**	0.8340	0.7657	0.7129	0.6733	0.6943

V. Discussion

In this paper a novel method for objective detection of additional feedback responses in human operator identification has been proposed. The methodology was applied to a multi-channel control task with additional controlled element output feedback provided by physical motion feedback or additional visual information. For identification, an ARX model-based method was applied, while the estimated models were evaluated using an objective model selection criterion proposed by Drop et al.[20] A human-in-the-loop experiment and offline simulations supplied the data to develop and tune this criterion to our specific application.

The offline Monte Carlo simulations were performed using human operator models matching the operator behavior observed in the experiment for direct comparison with the experiment results. A visual inspection of the resulting graphs and a evaluation based on coefficients of determination revealed that the simulation results corresponded to those of the experiment at noise intensity levels representative for human operator behavior. It should be noted that this analysis focused on the effect of the remnant power while the results are also influenced by a number of other factors, such as the relative contributions of the error and output responses. Nevertheless, this comparison is a valuable test for the method's applicability to experiment data.

The graphs generated for tuning the methodology revealed the probability of the presence of an additional operator response. The strength of the output response, that is the extent to which the human operator uses the available feedback, could be derived from this probability. For the no motion (C0) and one-to-one motion (C3) conditions the true dynamics were known beforehand, so these conditions served as a baseline. For the low-fidelity motion condition (C1) it was hypothesized that the H_{p_x} response would not be very pronounced, and this was found to indeed be the case. The strength of the output response was almost identical for the high-fidelity motion (C2) and one-to-one motion (C3) condition as was hypothesized beforehand. For the pursuit condition (P0) there was surprisingly little evidence for the existence of an additional operator response. Although an improvement in tracking performance was observed in earlier studies,[13,28] it remains uncertain whether the use of a multi-channel control organization and/or linear human operator models is suitable for capturing the dynamics in pursuit tracking tasks.

For the low-fidelity motion and the pursuit condition the existence of the H_{p_x} response appears to be highly unlikely, but the results are not distinct enough to identify an ideal value of the penalty parameter c. Therefore, the penalty parameter c included in the model selection criterion was only tuned for the no motion and high-fidelity motion conditions. A range of optimal c values was defined that would ensure identification of correct models. It should be noted that this choice is based on data from five participants, making the effect of one subject on the ideal range of c quite significant.

The range of optimal c values for the mBIC for our application ($3 < c < 10$) was found to be unexpectedly consistent with earlier findings for very different manual control tasks, focusing on human feedforward control with predictable target signals.[20] While this consistency suggests that an optimal c setting that is "universally" applicable to human operator identification may exist, only the variation in the data over our experiment conditions already shows that the choice for c is definitely not trivial and care should be taken in making any *a priori* assumptions for its value.[20]

The experiment in this study included a controlled element with unstable double-integrator dynamics to induce a strong output response. This type of control task is of little practical use as it is not representative for most realistic human control scenarios. More realistic controlled element dynamics that resemble those of a real aircraft could be implemented in the future to further test our methodology. It can already be hypothesized that for this type of task lower ideal c values will be found as the evidence for an H_{p_x} will presumably be weaker. Double-integrator dynamics

require considerable lead and thus, a strong state feedback. For "easier" aircraft dynamics less lead is needed, so the operator is likely to develop an overall weaker output response.

One possible further application of the methodology is similar to the one treated in this paper and also involves the detection of an additional operator response. Van der El et al.[31] proposed a model for preview tracking that includes a near-viewpoint feedforward response. The contribution of this additional response appeared to be very small, so our approach might be used to investigate the presence of the feedforward. Another possible application involves the inspection of the operator model structure itself rather than the number of responses. Pool et al.[32] proposes an extra lead-lag term in the human operator equalization transfer function to model human operator dynamics more realistically over a wide frequency range. In this case the objective model selection criterion could be used to identify the model orders and assess the applicability of the extended model.

VI. Conclusions

The intended purpose of the approach investigated in this paper was the objective detection of additional human operator responses in control tasks that contain additional physical or visual cues. The proposed method is based on linear-time invariant ARX models in combination with an objective model selection criterion. To test the effectiveness of the method, it was applied to experiment and simulation data. The analysis confirmed Drop et al.'s findings[20] that conventional model selection criteria such as the Bayesian information criterion cannot by applied to data from human-in-the-loop experiments without modification. Due to the relatively high remnant noise levels characteristic of human operator control behavior, a higher penalty has to be added to model complexity to prevent overfitting. A range of optimal penalty value that would ensure the identification of the correct number of operator responses was identified ($3 < c < 10$). The optimal penalty values could only be found for the compensatory no-motion control task and tracking tasks with high-quality motion feedback. The presence of an output response in conditions with low-fidelity motion feedback or in pursuit tracking tasks remains debatable.

The findings were verified by the results obtained from the offline analysis. Contrary to experiment data, there is no uncertainty with regard to the presence of the output response in the simulation data, as the number of operator responses is known from the simulation set-up. The match that was found between experiment and simulation results suggests that the same dynamics were identified, thereby increasing our confidence in the efficacy of the method. In future research, the approach presented in this paper may be used to study the utilization of additional human operator responses, and their modeling, in other applications.

References

[1]McRuer, D. T., Graham, D., Krendel, E. S., and Reisener, W. J., "Human Pilot Dynamics in Compensatory Systems, Theory Models and Experiments with Controlled Element and Forcing Function Variations," Tech. Rep. AFFDL-TR-65-15, Air Force Flight Dynamics Laboratory, Wright-Patterson Air Force Base (OH), 1965.

[2]McRuer, D. T. and Jex, H. R., "A Review of Quasi-Linear Pilot Models," *IEEE Transactions on Human Factors in Electronics*, Vol. HFE-8, No. 3, Sept. 1967, pp. 231–249.

[3]Hess, R. A., "Model for Human Use of Motion Cues in Vehicular Control," *Journal of Guidance, Control, and Dynamics*, Vol. 13, No. 3, 1990, pp. 476–482.

[4]Beerens, G. C., Damveld, H. J., Mulder, M., van Paassen, M. M., and van der Vaart, J. C., "Investigation into Crossover Regression in Compensatory Manual Tracking Tasks," *Journal of Guidance, Control, and Dynamics*, Vol. 32, No. 5, 2009, pp. 1429–1445.

[5]Mulder, M., Zaal, P. M. T., Pool, D. M., Damveld, H. J., and van Paassen, M. M., "A Cybernetic Approach to Assess Simulator Fidelity: Looking back and looking forward," *Proceedings of the AIAA Modeling and Simulation Technologies (MST) Conference*, No. AIAA 2013-5225, Boston (MA), August 19-22, 2013.

[6]Stapleford, R. L., Peters, R. A., and Alex, F. R., "Experiments and a Model for Pilot Dynamics with Visual and Motion Inputs," *NASA CR-1325*, 1969.

[7]van Paassen, M. M. and Mulder, M., "Identification of Human Operator Control Behavior in Multiple-Loop Tracking Tasks," *Proceedings of the Seventh IFAC/IFIP/IFORS/IEA Symposium on Analysis, Design and Evaluation of Man-Machine Systems*, Kyoto, Japan, September 16-18, 1998, pp. 512–520.

[8]Nieuwenhuizen, F. M., Zaal, P. M. T., Mulder, M., van Paassen, M. M., and Mulder, J. A., "Modeling Human Multichannel Perception and Control Using Linear Time-Invariant Models," *Journal of Guidance, Control, and Dynamics*, Vol. 31, No. 4, July-August 2008, pp. 999–1013.

[9]Zaal, P. M. T., Pool, D. M., Chu, Q. P., van Paassen, M. M., Mulder, M., and Mulder, J. A., "Modeling Human Multimodal Perception and Control Using Genetic Maximum Likelihood Estimation," *Journal of Guidance, Control, and Dynamics*, Vol. 32, No. 4, 2009, pp. 1089–1099.

[10]Hosman, R. J. A. W., *Pilot's Perception and Control of Aircraft Motions*, Ph.D. thesis, Delft University of Technology, 1996.

[11]van der Vaart, J. C., *Modelling of Perception and Action in Compensatory Manual Control Tasks*, Ph.D. thesis, Delft University of Technology, 1992.

[12]Wasicko, R. J., McRuer, D. T., and Magdaleno, R., "Human Pilot Dynamic Response in Single-loop Systems with Compensatory and Pursuit Displays," Tech. rep., AFFDL-TR-66-137, Air Force Flight Dynamics Laboratory, 1966.

[13]Vos, M. C., Pool, D. M., Damveld, H. J., van Paassen, M. M., and Mulder, M., "Identification of Multimodal Control Behavior in Pursuit Tracking Tasks," *Proceedings of the 2014 IEEE International Conference on Systems, Man, and Cybernetics*, San Diego (CA), October 5-8, 2014, pp. 69–74.

[14]Shirley, R. S. and Young, L. R., "Motion Cues in Man-Vehicle Control - Effects of Roll-Motion Cues on Human Operator's Behavior in Compensatory Systems with Disturbance Inputs," *IEEE Transactions on Man-Machine Systems*, Vol. 9, No. 4, 1968, pp. 121–128.

[15]Young, L. R., "Some Effects of Motion Cues on Manual Tracking," *Proceedings of the Second Annual NASA-University Conference on Manual Control*, Massachusetts Institute of Technology, Cambridge (MA), February 28 - March 2, 1966, pp. 231–240.

[16]Pool, D. M., Zaal, P. M. T., Damveld, H. J., van Paassen, M. M., and Mulder, M., "Evaluating Simulator Fidelity using In-Flight and Simulator Measurements of Roll Tracking Behavior," *Proceedings of the AIAA Modeling and Simulation Technologies Conference*, No. AIAA 2012-4635, Minneapolis (MN), August 13-16, 2012.

[17]Pool, D. M., van Paassen, M. M., and Mulder, M., "Effects of Motion Filter Gain and Break Frequency Variations on Pilot Roll Tracking Behavior," *Proceedings of the AIAA Modeling and Simulation Technologies Conference*, No. AIAA 2013-5224, Boston (MA), August 19-22, 2013.

[18]Pool, D. M., Harder, G. A., Damveld, H. J., van Paassen, M. M., and Mulder, M., "Evaluating Simulator-Based Training of Skill-Based Control Behavior using Multimodal Operator Models," *Proceedings of the 2014 IEEE International Conference on Systems, Man, and Cybernetics*, San Diego (CA), October 5-8, 2014, pp. 3868–3873.

[19]Pool, D. M., Harder, G. A., and van Paassen, M. M., "Effects of Simulator Motion Feedback on Training of Skill-Based Control Behavior," *Journal of Guidance, Control, and Dynamics*, Vol. 39, No. 4, 2016, pp. 889–902.

[20]Drop, F. M., Pool, D. M., van Paassen, M. M., Mulder, M., and Bülthoff, H. H., "Objective Model Selection for Identifying the Human Feedforward Response in Manual Control," *IEEE Transactions on Cybernetics*, Accepted for publication.

[21]Akaike, H., "A New Look at the Statistical Model Identification," *IEEE Transactions on Automatic Control*, Vol. AC-19, No. 6, 1974, pp. 716–723.

[22]Schwarz, G., "Estimating the Dimension of a Model," *The Annals of Statistics*, Vol. 6, No. 2, 1978, pp. 461–464.

[23]Valente Pais, A. R., Pool, D. M., de Vroome, A. M., van Paassen, M. M., and Mulder, M., "Pitch Motion Perception Thresholds During Passive and Active Tasks," *Journal of Guidance, Control, and Dynamics*, Vol. 35, No. 3, 2012, pp. 904–918.

[24]Lu, T., Pool, D. M., van Paassen, M. M., and Mulder, M., "Use of Simulator Motion Feedback for Different Classes of Vehicle Dynamics in Manual Control Tasks," *Proceedings of the 5th CEAS Air & Space Conference, Delft, The Netherlands*, No. 52, Sept. 2015.

[25]Drop, F. M., Pool, D. M., Damveld, H. J., van Paassen, M. M., and Mulder, M., "Identification of the Feedforward Component in Manual Control With Predictable Target Signals," *IEEE Transactions on Cybernetics*, Vol. 43, No. 6, December 2013, pp. 1936–1949.

[26]Ljung, L., *System Identification Theory for the User*, Prentice-Hall, Upper Saddle River, NJ, 2nd ed., 1999.

[27]Berkouwer, W. R., Stroosma, O., van Paassen, M. M., Mulder, M., and Mulder, J. A., "Measuring the Performance of the SIMONA Research Simulator's Motion System," *Proceedings of the AIAA Modeling and Simulation Technologies Conference and Exhibit*, No. AIAA 2005-6504, San Francisco (CA), August 15-18, 2005.

[28]Praamstra, F. J., Zaal, P. M. T., Pool, D. M., Ellerbroek, J., Mulder, M., and van Paassen, M. M., "Function of Attitude Perception in Human Control Behavior in Target Tracking Tasks," *Proceedings of the AAIA Modeling and Simulation Technologies Conference and Exhibit*, No. AIAA 2008-6845, Honolulu (HI), August 18-21, 2008.

[29]Pool, D. M., Mulder, M., van Paassen, M. M., and van der Vaart, J. C., "Effects of Peripheral Visual and Physical Motion Cues in Roll-Axis Tracking Tasks," *Journal of Guidance, Control, and Dynamics*, Vol. 31, No. 6, 2008, pp. 1608–1622.

[30]Zaal, P. M. T., Popovici, A., and Zavala, M. A., "Effects of False Tilt Cues on the Training of Manual Roll Control Skills," *Proceedings of the AIAA Modeling and Simulation Technologies Conference, Kissimmee (FL)*, No. AIAA-2015-0655, 2015.

[31]van der El, K., Pool, D. M., Damveld, H. J.and van Paasen, M. M., and Mulder, M., "An Empirical Human Controller Model for Preview Tracking Tasks (2015)," *IEEE Transactions on Cybernetics*, online preprint available.

[32]Pool, D. M., Zaal, P. M. T., Damveld, H. J., van Paassen, M. M., van der Vaart, J. C., and Mulder, M., "Modeling Wide-Frequency-Range Pilot Equalization for Control of Aircraft Pitch Dynamics," *Journal of Guidance, Control, and Dynamics*, Vol. 34, No. 5, September-October 2011, pp. 1529–1542.

A. Appendix: Human Operator Model Parameters

Fig. 10 shows the parameters that were estimated for each condition and subject using the time-domain human operator fitting procedure of Ref. 9. The errorbars indicate the 95% confidence intervals and black markers show the averages over the five participants. The average parameters for each condition were used in the offline analysis.

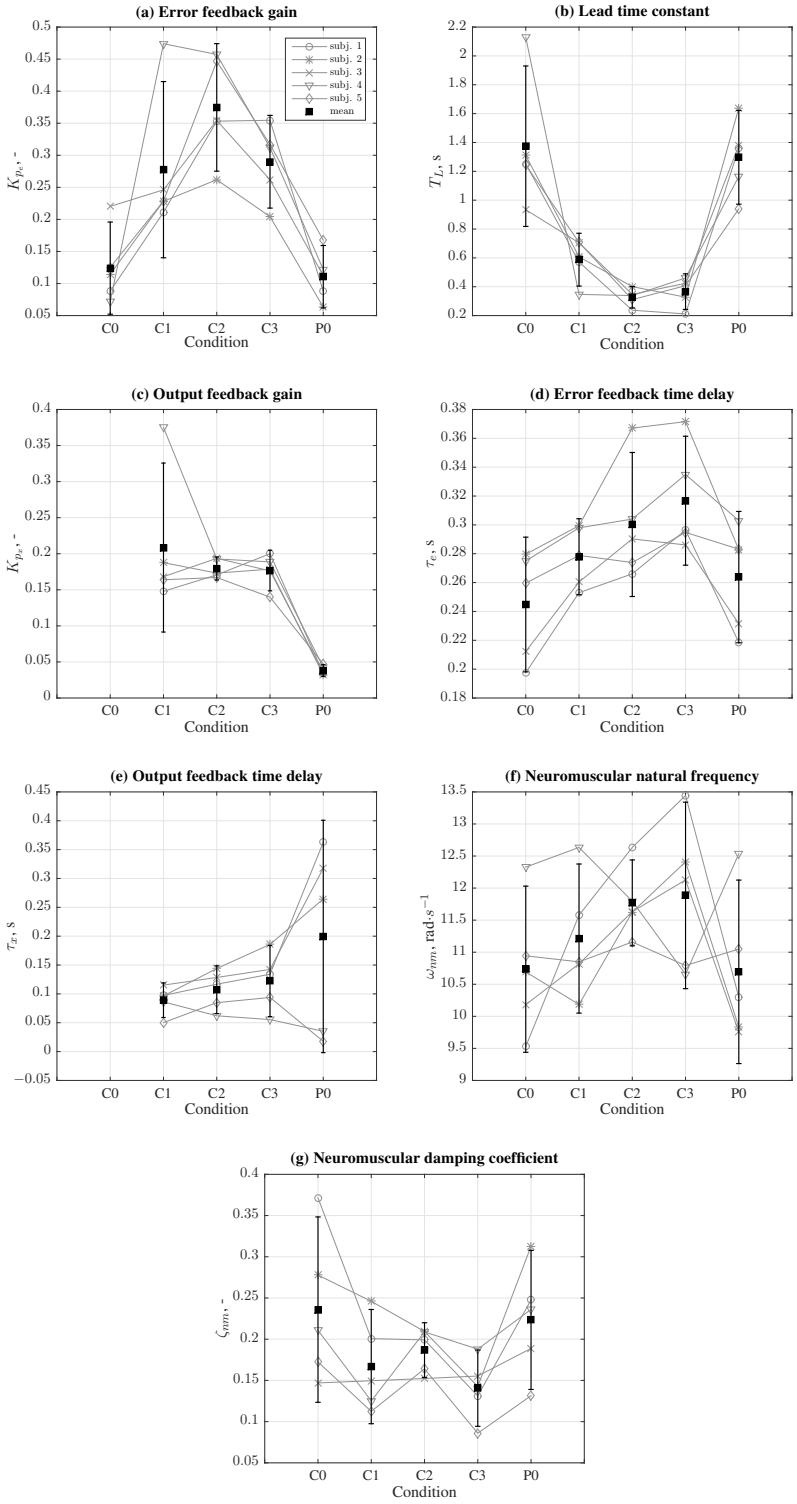

Figure 10. Human operator model parameters estimated from the human-in-the-loop experiment data.